IL NUOVO CIMENTO Vol. 34 C, N. 5 Settembre-Ottobre 2011
DOI 10.1393/ncc/i2011-10924-8

Colloquia: SIF Congress 2010

Preliminary study of the ^{19}F(^{7}Li, ^{7}Be)^{19}O reaction at 52 MeV with MAGNEX

M. Cavallaro

INFN, Laboratori Nazionali del Sud - via S. Sofia 62, 95125 Catania, Italy

(ricevuto il 23 Dicembre 2010; revisionato il 24 Gennaio 2011; approvato il 24 Gennaio 2011; pubblicato online il 2 Agosto 2011)

Summary. — The ^{19}F(^{7}Li, ^{7}Be)^{19}O charge-exchange reaction at 52.2 MeV incident energy has been studied at the INFN-LNS laboratory in Catania (Italy) using the MAGNEX spectrometer. Thanks to an algebraic ray-reconstruction technique and to a high-performing focal plane detector, high-resolution ^{19}O energy spectra and angular distributions have been extracted. A theoretical analysis of the reaction in the framework of the Charge-Exchange Quasiparticle Random Phase Approximation (CEX-QRPA) has been done. The results of Distorted-Wave Born Approximation (DWBA) calculations in a double folding scheme have been compared to the experimental angular distribution of the transition to the ^{19}O state at 1.47 MeV state and show a remarkable agreement both in magnitude and shape.

PACS 25.70.Kk – Charge-exchange reactions.
PACS 21.10.Pc – Single-particle levels and strength functions.
PACS 29.30.Ep – Charged-particle spectroscopy.

1. – Introduction

The Charge-EXchange (CEX) reactions have represented, over the last decades, the major source of information on isovector excitations in light-stable and weakly bound nuclei. Beside the interest as spectroscopic tools, studies on CEX reactions like (p, n) or (n, p) also give useful information on the response function of nuclei to the isovector component of the effective nucleon-nucleon interaction [1, 2]. CEX reactions involving heavy-ion projectiles have been useful to obtain complementary information about states which are not easily excited with elementary probes [3, 4]. This includes the excitation of high-spin states in the very peripheral collisions or the selection of Fermi (F) or Gamow-Teller (GT) transitions by an appropriate choice of projectile-target combinations.

A the same time, the CEX reactions have allowed the study of nuclear structure and reaction dynamics far off the stability valley, giving the possibility to explore new and exciting phenomena characteristic of those systems. In such studies, a crucial role has

been played by the use of magnetic spectrometers to detect the ejectiles at forward angles and with high-energy resolution.

A systematic exploration of the structural properties of a particular category of light neutron-rich nuclei, for which an inner core of an integer number of α-particles is coupled to three external neutrons ($N\alpha + 3$ neutrons) has been performed in the last years. Such studies on nuclei belonging to this category as ^{11}Be and ^{15}C [5, 6] have shown that the (^{7}Li, ^{7}Be) reaction at about 8 MeV/u incident energy is a suitable tool to explore such systems. In fact, it has been demonstrated that this process proceeds with a considerable predominance of the direct one-step mechanism in such energy range, thus being a useful probe for spectroscopic studies. A research campaign on (^{7}Li, ^{7}Be) reactions in these conditions has been realized at the IPN-Orsay Tandem laboratory by using the Enge Split-Pole spectrometer [7]. It was then continued at the Catania INFN-LNS laboratory where, thanks to the availability of the MAGNEX large-acceptance spectrometer, it was possible to study the (^{7}Li, ^{7}Be) reaction down to 1 μb/sr or less, thus extending the systematic study to heavier nuclei, where the cross-sections are typically smaller [8].

In particular, the analysis of the transition to the state at 1.47 MeV of the ^{19}O nucleus populated via the (^{7}Li, ^{7}Be) reaction at 52.2 MeV incident energy is presented in this paper. Excitation energy spectra and angular distributions, even if characterized by low cross-sections, have been measured for the first time thanks to the high performance of the MAGNEX spectrometer. A theoretical analysis based on the CEX-QRPA semi-microscopic approach has been developed and is presented in the paper.

2. – The reaction mechanism

A well-defined and nuclear-structure–independent proportionality between (p, n) or (n, p) reaction cross-sections and beta-decay transitions strength has been recognized since long [9]. Such a relationship is very useful allowing beta-transition strength functions to be mapped out of excitation energy regions that are energetically accessible to beta-decay. Moreover, an accurate empirical link between (p, n) or (n, p) cross-sections and the well-known beta-decay process would put our understanding of the nucleon-nucleon force and nuclear reaction mechanism on a firmer quantitative footing.

A number of studies [10] have investigated the properties of the isovector effective interaction using the correspondence between beta-decay and (p, n) or (n, p) reactions already in the late 1950's. Since the momentum transfer (q) in beta-decay is small, the transition amplitude for the (p, n) or (n, p) reactions should be evaluated for $q \approx 0$, *i.e.* near the scattering angle $\theta_{lab} = 0^\circ$. Moreover, since the proportionality between beta-decay strengths and CEX cross-sections arises from the similarity between the spin and isospin structure of the central part of the nuclear effective interaction and the beta matrix elements, conditions with negligible contributions from the non-central parts have to be considered in order to achieve the proportionality. It is expected that spin-orbit and tensor components of the effective interaction can be neglected in the limit $q \approx 0$. Thus for the (p, n) or (n, p) reaction cross-section near $\theta_{lab} = 0^\circ$, the analogy with beta-decay can be expressed with the following proportionality statement [11] connecting the reaction cross-section ($\mathrm{d}\sigma/\mathrm{d}\Omega$) with the beta-decay strength (B):

$$\frac{\mathrm{d}\sigma}{\mathrm{d}\Omega}(\alpha, q = 0) = \hat{\sigma}(E_p, A)B(\alpha). \tag{1}$$

Here α labels a particular transition channel (Fermi or Gamow-Teller type) and the proportionality factor $\hat{\sigma}$ is the measured ratio $\mathrm{d}\sigma/\mathrm{d}\Omega(q=0)/B$ for an appropriate transition of known beta-decay strength. This factor is called "unit cross-section" and can depend on the bombarding energy (E_p) and the target (A).

Several experimental difficulties raise to carry out CEX reactions with light projectiles as (n,p), $(d,{}^{2}\mathrm{He})$, $(t,{}^{3}\mathrm{He})$. For example, it is very difficult to produce a well-collimated and monochromatic neutron beam, and also typical neutrons intensities are small compared to charged particles beams. Triton beams could give rise to serious problems of radiation contamination and have typically low intensities, therefore they are not suitable to induce reactions characterized by low cross-sections. In the $(d,{}^{2}\mathrm{He})$ reaction, the break-up of deuterons is the most probable reaction channel and correlated pairs of particles are accompanied by a substantial proton background. Moreover, this reaction is characterized by the population of states with only pure spin-flip transition ($\Delta S = 1$), so that the excitations of scalar modes in the studied system is not allowed.

Heavy-ion–induced charge-exchange reactions can provide quantitative measurements of isovector excitations without the mentioned experimental problems. However, there are other problems which sometimes limit the usefulness of these reactions. The momentum transfer q increases rapidly with scattering angle with the result that the angular distributions are compressed into an angular range of a few degrees near $\theta_{lab} = 0^{\circ}$, and angular distributions for different ΔL transfers can be difficult to discriminate. Another drawback of heavy-ion CEX reactions is that multi-step processes, in which the same final states are populated by sequential proton-neutron or neutron-proton transfer reactions, can become dominant with respect to the direct ones, making it difficult to obtain clear information about the populated states. Moreover, for CEX reactions with heavy projectiles, the effects due to the internal structure of the colliding systems play an important role, making the interpretations of the data less straightforward. Characteristics of a particular heavy-ion CEX reaction are the selection rules on the angular momentum, depending on the structure of projectile and ejectile. For example, the $(^{12}\mathrm{C}, ^{12}\mathrm{N})$ reaction proceeds via GT dynamics for bombarding energies greater than 50 MeV/u, giving a simple interpretation of the angular distributions [12]. In this case the Fermi-like transitions are inhibited. Instead the $(^{13}\mathrm{C}, ^{13}\mathrm{N})$ reaction can proceed via the 0^{+} and 1^{+} dynamics. Moreover, ^{12}N and ^{13}N do not have any bound states other than the ground state, providing a clean determination of the excitation energy spectra of the product system. Instead, the $(^{14}\mathrm{C}, ^{14}\mathrm{N})$ is more complicated because of the many bound states of ^{14}N which may appear in the excitation energy spectra. Reactions as the $(^{16}\mathrm{O}, ^{16}\mathrm{F})$ with unbound ejectile are not suitable because they mainly proceed via three-body dynamics.

Among the heavy-ion–induced charge-exchange reactions with isospin selectivity $\Delta T_z = +1$, the $(^{7}\mathrm{Li}, ^{7}\mathrm{Be})$ reaction is considered a very useful tool for the investigation of nuclear isovector excitations. Since ^{7}Be presents a ground state ($3/2^{-}$, g.s.) and a bound excited state ($1/2^{-}$, 0.43 MeV), the reaction can easily proceed via the $(^{7}\mathrm{Li}_{3/2^{-}}, ^{7}\mathrm{Be}_{3/2^{-}})$ or the $(^{7}\mathrm{Li}_{3/2^{-}}, ^{7}\mathrm{Be}_{1/2^{-}})$ branch, characterized by different nucleonic spin transfer: 0^{+}, 1^{+}, 2^{+}, 3^{+} through the $^{7}\mathrm{Be}_{3/2^{-}}$ channel or 1^{+}, 2^{+} through the $^{7}\mathrm{Be}_{1/2^{-}}$ channel. Experimentally, if the energy resolution is better than 0.43 MeV or the deexcitation γ-rays for bound states are tagged, the two contributions can be separated. Because of the number of possible spin transfers, the interpretation of the angular distributions can be difficult. Anyway, the possibility to have the two routes turns out to be an important aspect, making the measurement of both spin-flip and non–spin-flip transitions possible.

People have been interested in using such reaction also because ^{7}Li and ^{7}Be are specular nuclei. The Q-values for these reactions are normally smaller than other CEX reactions, as for example (^{12}C, ^{12}N), because the contribution from the projectile side is small. As regards the matrix elements for the projectile transition, one should notice that the beta-transitions connecting ^{7}Be (ground and first excited state) with ^{7}Li are super-allowed ones. One of the likely consequences is the lower value of bombarding energy necessary for the dominance of the direct contribution over the two-step ones.

The problem to search whether and under which experimental conditions the direct process is dominant over two-step mechanisms was faced also for the (^{7}Li, ^{7}Be) reaction. An analysis to investigate how the (^{7}Li, ^{7}Be) mechanism develops, as the incident energy is changed, was done in the ^{12}C(^{7}Li, ^{7}Be)^{12}B reaction by Nakayama *et al.* [13]. The authors found that, by increasing the energy, the one-step curves increases except for the 3^- and 4^- states, where the direct mechanism is inhibited because of the high-angular moment involved. The fact that the experimental point at lower energy was not compatible with the theoretical curves for the direct mechanism was interpreted as a proof that the reaction proceeds via a two-step mechanism below 21 MeV/u.

Completely different conclusions were drawn by Etchegoyen *et al.* [14] measuring the ^{10}B(^{7}Li, ^{7}Be)^{10}Be reaction at 39 MeV. They performed calculations using a microscopic DWBA with both central and tensor forces and concluded that even at such low bombarding energies the one-step process results very important and the two-step mechanism is suppressed. Similar results come from the work by Cappuzzello *et al.* [5, 6] where the ^{11}B(^{7}Li, ^{7}Be)^{11}Be and ^{15}N(^{7}Li, ^{7}Be)^{15}C reactions were performed at 57 MeV incident energy and ^{11}Be and ^{15}C excitation energy spectra and angular distributions were extracted. The ^{16}O(^{7}Li, ^{7}Be)^{16}N reaction has been investigated at 50 MeV by Cook *et al.* [15] and the data were analyzed including calculations of both the direct reaction in a microscopic DWBA model and the sequential processes with coupled reaction channel (CRC) calculations [16]. Although a number of questions arise about the approximations made and the effects neglected within the CRC calculations, it was found that for transitions to unnatural parity states the direct process remains dominant, while for transitions to natural parity states, the sequential contribution, in particular the (^{7}Li, ^{6}Li)(^{6}Li, ^{7}Be) process, becomes important.

As a consequence, according to the present knowledge about CEX dynamics, one can conclude that, while the competition of one-step and two-step CEX routes was found to be important for reactions with an incident ^{12}C projectile at low energies [3, 4], this seems not the case of (^{7}Li, ^{7}Be) reactions. The observed suppression of two-step processes in (^{7}Li, ^{7}Be) reactions at low energies is very likely related to the fact that unbound intermediate states (^{8}Be) are involved. Since the overlap between their wave functions (typically large in the position representation) with the localized configurations of the bound initial and final states is small, the two-step amplitudes as a whole seem to be reduced. This motivation increases when also the product nuclei involved are weakly bound, as in the case of the ^{11}Be or ^{15}C.

3. – Experimental setup

The ^{19}F(^{7}Li, ^{7}Be)^{19}O reaction has been performed at INFN-Laboratori Nazionali del Sud (LNS). The ^{7}Li^{+++} beam at 52.2 MeV was delivered by the Tandem accelerator. The target containing ^{19}F was a 80 μg/cm^2 AlF_3 foil evaporated on a 250 μg/cm^2 gold backing produced at the chemical laboratory of the LNS. A self-supporting ^{27}Al target (116 μg/cm^2) was also used in order to estimate the aluminium presence in the target

compound and subtract it in the final spectra. Supplementary runs were done also on a WO_3 target ($150\,\mu g/cm^2$ thick on $20\,\mu g/cm^2$ carbon backing) and on a carbon target ($76\,\mu g/cm^2$) for the subtraction of the contribution due to the oxygen and carbon impurities in the AlF_3 target.

The reaction ejectiles were momentum analyzed by the MAGNEX large-acceptance magnetic spectrometer and detected by its Focal Plane Detector (FPD) [8, 17]. The MAGNEX quadrupole and dipole fields and the α-surface coil, together with the positioning of the FPD, were set in order to focus the ^{7}Be ejectiles relative to the $^{19}O_{g.s.}$ in the focal plane position corresponding to a momentum deviation +8% with respect to the central trajectory.

The optical axis of the spectrometer was centred at an angle $\theta_{opt} = 12.2^\circ$ in the laboratory with respect to the beam incidence direction. Thanks to the large angular-acceptance of MAGNEX (horizontally -0.090 rad, $+0.110$ rad, vertically ± 0.125 rad in the spectrometer reference frame), an angular range between about 7° and 19° has been explored in a unique setting of the spectrometer.

4. – Experimental data analysis

The beryllium isotopes have been identified by the FPD using the simultaneous measurement of their position at the focal plane and their residual energy by the hodoscope of silicon detectors. Recently it has been shown that this technique allows a clear identification of the different detected ions with a mass resolution as high as 1/160 [18]. Once the ^{7}Be ejectiles are selected, the measured horizontal and vertical positions and angles at the focal plane are analyzed [8, 17].

Using an algebraic ray-reconstruction technique, the final coordinates of the detected ions measured at the focal plane were related to the initial ones at the target point. Such technique, based on the formalism of differential algebra [19, 20], is a perturbative method to solve the differential equations describing the motion of each ion through the spectrometer and to obtain the Taylor coefficients of the flow linking the initial phase space with the final one. In this mathematic environment, the integration of the differential equations results in a much simpler algebraic task and very high order of the perturbation series can be treated. In practice, thanks to this technique, if the positions and angles of the detected ions are determined by an accurate measurement at the focal plane, the full trajectories back to the reaction target can be reconstructed and consequently the initial momentum vector (scattering angles and excitation energies) of the reaction products is obtained by the application of the inverse map to the measured phase space parameters [21].

In fig. 1 a reconstructed spectrum of the ^{19}O excitation energy is shown for the angular range $9.5^\circ < \theta_{lab} < 13.5^\circ$. The spectrum is obtained from the data on the AlF_3 target. The aluminium target histogram is also shown superimposed. The same histogram with the subtraction of the normalized contribution related to the aluminium target is shown in fig. 2. At excitation energies larger than 6 MeV also the contribution due to the presence of ^{12}C and ^{16}O in the target should be considered and the analysis is on the way.

Several excited states are observed and identified in the low excitation energy region. Most of the ^{19}O states have been observed in the past by one and two neutron transfer reactions [22], thus confirming the capability of the (^{7}Li, ^{7}Be) reactions to populate such states. For example, the shell structure configuration of the 1.47 MeV excited state ($1/2^+$) is quite well known. It is mainly a single-particle state with the configuration of

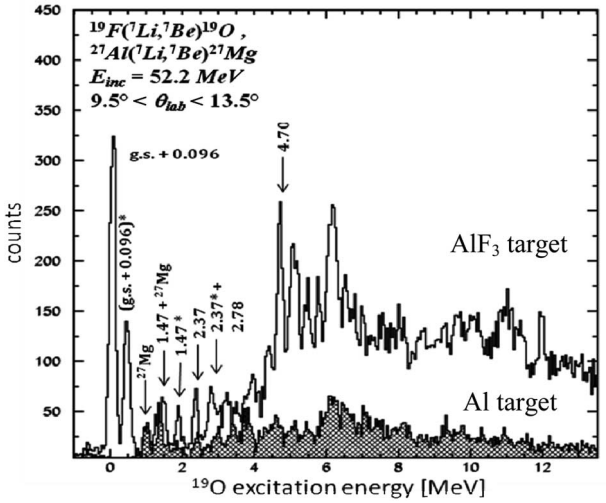

Fig. 1. – ^{19}O excitation energy spectrum obtained from the ^{19}F(^{7}Li, ^{7}Be)^{19}O reaction at 52.2 MeV on AlF_3 target and on Al target in the angular range $9.5^\circ < \theta_{lab} < 13.5^\circ$. Some of the known ^{19}O states are indicated with their energy. Peaks marked with an asterisk refer to the transitions in which the ^{7}Be ejectiles are in the first excited state at 0.43 MeV.

one neutron in the $2s_{1/2}$ orbital on a ^{18}O(0^+) core. The transition from the ^{19}F (g.s., $1/2^+$) to this state can proceed via 0^+ or 1^+ spin transfer.

One of the advantage of working with a large acceptance spectrometer is that, in a unique setting of the instrument, a wide range of scattering angles can be explored.

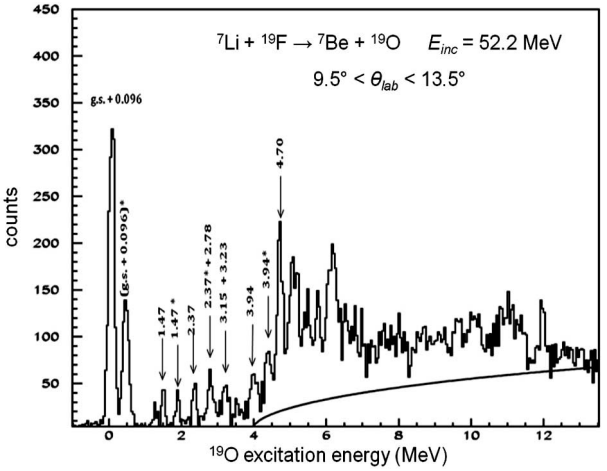

Fig. 2. – ^{19}O excitation energy spectrum obtained from the ^{19}F(^{7}Li, ^{7}Be)^{19}O reaction at 52.2 MeV. The contribution due to the Al presence in the target has been subtracted. The solid line is the estimated three-body phase space $^7\mathrm{Li} + {}^{19}\mathrm{F} \rightarrow {}^7\mathrm{Be} + {}^{18}\mathrm{O} + \mathrm{n}$. The known ^{19}O states are indicated with their energy. Peaks marked with an asterisk refer to the transitions in which the ^{7}Be ejectiles are in the first excited state at 0.43 MeV.

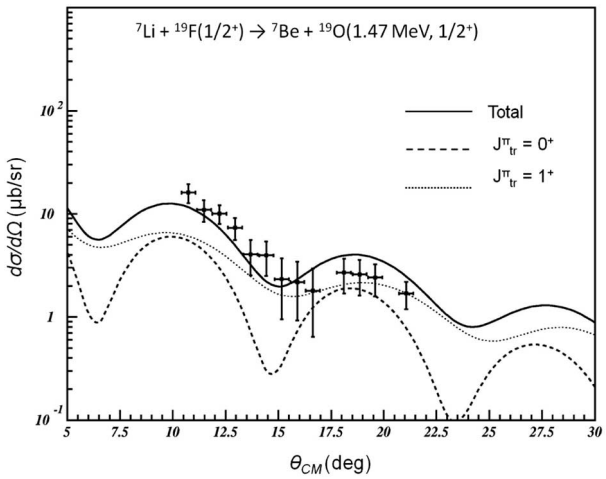

Fig. 3. – Calculated angular distribution for the ^{19}F(^{7}Li, ^{7}Be)^{19}O$_{1.47}$ transition (solid line). The two contributions due to the 0^+ and 1^+ target transitions are shown separately (dashed lines). The calculated cross-sections are not scaled. The experimental angular distribution is also shown.

As a consequence, a consistent part of the cross-section angular distribution can be measured in a single run in the same experimental conditions, resulting in a reduction of the uncertainty due to the normalization of runs at different angles. In the present case, a single set of measurements with the spectrometer optical axis centred at $\theta_{opt} = 12.2^\circ$ allows to obtain an angular distribution for scattering angles between about $10^\circ < \theta_{CM} < 21^\circ$ in the centre of mass. The measured angular distribution for the transition to the ^{19}O (1.47 MeV, $1/2^+$) excited state is shown in fig. 3. The error bars are estimated by taking into account the statistical contribution on the number of counts.

5. – Theoretical calculations

A theoretical analysis of the ^{19}F(^{7}Li, ^{7}Be)^{19}O reaction in the framework of the CEX-QRPA [12, 23] has been done. As the usual RPA, it is based on a mean field approach with the inclusion of 1p-1h (2QP) correlations, but it also takes into account a description of the state-dependent pairing field felt by quasiparticles and an average treatment of the 2p-2h (4QP) particle configurations, normally not considered in the QRPA problem.

The CEX-QRPA approach is used to extract both structure and reaction information. It allows in fact to describe the ^{19}O level densities and to calculate the transition densities connecting the ^{19}F ground state to the 1p-1h excited states of ^{19}O. Such quantities are then introduced in double folding based form factors, thus allowing a direct connection to reaction cross-section calculations by a suitable DWBA. Consistency between structure and reaction calculation is achieved through the use of the same effective nucleon-nucleon interaction in each step of the calculations. In fact, following the semi-phenomenological approach of refs. [24,25], both the static mean field and pairing interaction for the QRPA derive from the same D3Y interaction of Hoffman and Lenske [24], which is also used to build the double folding integral used as optical potential in the DWBA calculations.

This approach is well suited for light neutron-rich nuclei, since it already succeeded in describing both the ^{11}B(^{7}Li, ^{7}Be)^{11}Be and the ^{15}N(^{7}Li, ^{7}Be)^{15}C reactions without change of the basic parameters [5, 6].

In fig. 3, the experimental angular distribution for the transition to the $^{19}O_{1.47}(1/2^+)$ state is shown together with the results of the QRPA-DWBA calculations for the two different multipolarity 0^+ and 1^+ allowed from the ^{19}F(g.s., $1/2^+$) target. The incoherent sum of the cross-section contributions of the two target transitions is also shown. The calculations satisfactorily describe the magnitude of the measured cross-section, without the need of introducing any renormalization factor ($N_{th} = 1$). This is a noticeable result since usually large scaling factors (even one order of magnitude) in the calculated cross-sections have been used to reproduce the experimental data from the (^{7}Li, ^{7}Be) reactions [26-28]. The close agreement is mainly due to the realistic description of the interaction [24] used in the form factor calculations, which has already shown to be appropriate for light neutron-rich nuclei at low energy [12, 29, 30]. This also demonstrates the reliability of a one-step approach in such conditions.

The general shape of the experimental angular distribution is also well reproduced. This supports the assumption of $1/2^+$ single-particle configuration with one neutron in the $2s_{1/2}$ orbital for such state, as reported in the literature [31].

6. – Conclusions

The ^{19}F(^{7}Li, ^{7}Be)^{19}O reaction has been studied at 52.2 MeV incident energy and at forward angles using the MAGNEX spectrometer. Thanks to the large energy acceptance (about ±25%), the ^{19}O excitation energy spectrum has been explored up to 14 MeV with a single setting of the magnetic fields. The use of supplemental targets has enabled to estimate the contribution in the spectra due to the presence of impurities in the AlF_3 target and to clearly identify the ^{19}O excited states at least at low excitation energy. The large angular acceptance of MAGNEX (about 50 msr) has allowed the extraction of the cross-sections in a quite wide angular range with a unique setting of the spectrometer angle.

The ^{19}O 1.47 MeV state has been specifically analysed by a microscopic approach based on QRPA-derived transition densities. The model is based on the calculation of the 1p-1h correlations on a HFB mean field in a broad phase-space extending far in the continuum. A microscopically derived D3Y interaction included in the model does not allow for any *a priori* adjustment of the parameters, resulting in a powerful scheme for the calculations. The QRPA model could describe rather well states with large 1p-1h configuration. The calculated transition densities have been then introduced in the double-folding integrals giving the charge-exchange form factors and the cross-sections, calculated in one-step DWBA approach. The case of the $^7\text{Li} + {}^{19}\text{F}(\text{g.s.}, 1/2^+) \rightarrow {}^7\text{Be} + {}^{19}\text{O}^{1.47}(1/2^+)$ transition has shown a good agreement with the experimental data, both in the shape of the angular distribution and in the magnitude of the cross section, without introducing any renormalization factor.

From all these results one can draw a two-fold conclusion: i) MAGNEX has proved to be able to provide results of physical interest, even in condition of low cross-sections ($< 10\,\mu$b/sr). ii) The experimental results seem to confirm the validity of the assumption of one-step mechanism for the (^{7}Li, ^{7}Be) reaction at about 8 MeV/u, providing that a fully microscopic approach is used to analyze the data. This behaviour, already observed for the ^{11}Be and ^{15}C cases studied in this way, strengthens the conclusions drawn in such works, opening a new scenario on the application of (^{7}Li, ^{7}Be) reactions

as tool to determine GT strength for neutron-rich systems, where β-decay data are not accessible.

* * *

I would like to thank the whole MAGNEX group and in particular F. Cappuzzello for their efforts in the years that has allowed to perform the experiment and to make the very complex data reduction and analysis. I also thank H. Lenske for the theoretical support in the understanding of the phenomena and in the developing of the analysis.

REFERENCES

[1] Alford W. P. *et al.*, *Adv. Nucl. Phys.*, **24** (1998) 1.
[2] Osterfeld F., *Rev. Mod. Phys.*, **64** (1992) 491.
[3] Bohlen H. G. *et al.*, *Nucl. Phys. A*, **488** (1988) 89c.
[4] Lenske H. *et al.*, *Phys. Rev. Lett.*, **62** (1989) 1457.
[5] Cappuzzello F. *et al.*, *Nucl. Phys. A*, **739** (2004) 30.
[6] Orrigo S. E. A. *et al.*, *Phys. Lett. B*, **633** (2006) 469.
[7] Nociforo C. *et al.*, *Eur. Phys. J. A*, **27**, s01 (2006) 283.
[8] Cavallaro M., *First Application of the MAGNEX Spectrometer: Investigation of the* ^{19}F(^{7}Li, ^{7}Be)^{19}O *reaction at* 52 MeV, PhD Thesis, University of Catania (2009).
[9] Bloom S. *et al.*, *Phys. Rev. Lett.*, **3** (1959) 98.
[10] Wisscher W. M. *et al.*, *Phys. Rev.*, **107** (1957) 781.
[11] Taddeucci T. N. *et al.*, *Nucl. Phys. A*, **469** (1987) 125.
[12] Lenske H., *Nucl. Phys. A*, **482** (1988) 343.
[13] Nakayama S. *et al.*, *Phys. Lett. B*, **246** (1990) 342.
[14] Etchegoyen A. *et al.*, *Phys. Rev. C*, **38** (1988) 2124.
[15] Cook J. *et al.*, *Phys. Rev. C*, **30** (1984) 1538.
[16] Clarke N. M. and Cook J., *Nucl. Phys. A*, **458** (1986) 137.
[17] Boiano C. *et al.*, *IEEE Trans. Nucl. Sci.*, **55** (2008) 3563.
[18] Cappuzzello F. *et al.*, *Nucl. Instrum. Methods A*, **621** (2010) 419.
[19] Berz M., *AIP Conf. Proc.*, **249** (1991) 456.
[20] Makino K. and Berz M., *Nucl. Instrum. Methods A*, **427** (1999) 338.
[21] Cappuzzello F. *et al.*, *Nucl. Instrum. Methods A*, **638** (2011) 74.
[22] Wiza J. L. *et al.*, *Phys. Rev.*, **143** (1966) 676.
[23] Ring P. and Shuck P., *The nuclear many-body problem* (Springer) 1980.
[24] Hoffmann F. *et al.*, *Phys. Rev. C*, **57** (1998) 2281.
[25] Baker F. T. *et al.*, *Phys. Rep.*, **289** (1997) 235.
[26] Bang J. *et al.*, *Nucl. Phys. A*, **429** (1984) 330.
[27] Cook J. and Kemper K. W., *Phys. Rev. C*, **30** (1984) 1538.
[28] Nakayama S. *et al.*, *Nucl. Phys. A*, **507** (1990) 515.
[29] Lenske H. *et al.*, *Prog. Part. Nucl. Phys.*, **46** (2001) 187.
[30] Cappuzzello F. *et al.*, *Europhys. Lett.*, **65** (2004) 766.
[31] Ajzenberg-Selove F., *Nucl. Phys. A*, **490** (1988) 1.